

Levetiracetam analogs: chemoenzymatic synthesis, absolute configuration assignment and evaluation of cholinesterase inhibitory activities

Cintia Duarte de Freitas Milagre^{1+✉}, Bruno Sergio do Amaral^{1✉}, João Marcos Batista Junior^{2,3✉}, Adriana Ferreira Lopes Vilela^{4✉}, Carmen Lúcia Cardoso^{4✉}, Humberto Marcio Santos Milagre^{1✉}

1. São Paulo State University, Institute of Chemistry, Araraquara, Brazil.
2. Federal University of São Carlos, Department of Chemistry, São Carlos, Brazil.
3. Federal University of São Paulo, Institute of Science and Technology, São José dos Campos, Brazil.
4. University of São Paulo, Faculty of Philosophy, Sciences and Letters, Ribeirão Preto, Brazil.

+Corresponding author: Cintia Duarte de Freitas Milagre, **Phone:** +55 16 33019668, **Email address:** cintia.milagre@unesp.br

ARTICLE INFO

Article history:

Received: July 19, 2021

Accepted: September 14, 2021

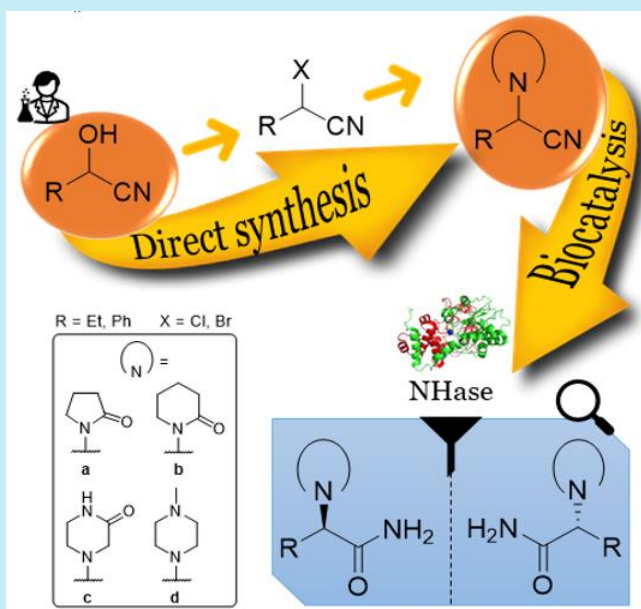
Published: April 01, 2022

Keywords

1. *N*-heterocycles
2. *N*-alkylation
3. biocatalysis
4. electronic circular dichroism (ECD)

Section Editor: Assis Vicente Benedetti

ABSTRACT: A chemoenzymatic approach for the synthesis of α -*N*-heterocyclic ethyl- and phenylacetamides, levetiracetam analogs, is described. Eight nitrile substrates were prepared through the *N*-alkylation of heterocycles (2-pyrrolidinone, 2-piperidinone, 2-oxopiperazine and 1-methylpiperazine) directly from hydroxyl group of ethyl and phenyl α -hydroxynitriles with yield of 35–71% after 12 h. Twenty nitrile hydratases (NHases) were screened and showed that the *N*-derivatives lactam substrates led to their correspondent amides by Co-type NHase with conversion and enantiomeric excess of up to 47.5 and 52.3% for (*S*)-enantiomer, while the piperazine substrates underwent spontaneous decomposition by retro-Strecker reaction. In order to avoid a retro-Strecker reaction of α -aminonitriles, ionic liquids and polyethylene glycol (PEG₄₀₀) were evaluated as alternative green solvents to aqueous buffered solutions in different proportions. Temperature was another parameter investigated during reaction-medium engineering for process optimization. However, unconventional reaction media and low temperature significantly reduced the NHase activity. The absolute configuration of α -*N*-heterocyclic ethyl- and phenylacetamides, some of which were new compounds, was determined using electronic circular dichroism (ECD) spectroscopy. Additionally, their potential as cholinesterase's inhibitors was evaluated.



1. Introduction

N-heterocycles are a key structural unit, which are vastly distributed among natural products and biomolecules, such as DNA and RNA, and correspond to more than 70% of all pharmaceuticals and agrochemicals (Liu *et al.*, 2019; Saini *et al.*, 2013). In addition, they play an important role in materials science, photonics, supramolecular and polymer chemistry (Chen *et al.*, 2019; Hong *et al.*, 2016). Therefore, given their importance, there is an increasing interest in synthesizing compounds bearing an *N*-heterocyclic scaffold. An interesting example in pharmaceuticals is levetiracetam (((2*S*)-2-oxopyrrolidin-1-yl)butanamide, Keppra) (Fig. 1), an antiepileptic drug that contains a pyrrolidinone unit and is commercialized by UCB Pharma, with sales over € 790 million in 2018, where € 221 million corresponded to the US market, € 216 million to the European market and € 352 million to international markets. Its patent in Japan expired in 2020, which impacted the US sales net by generic competition (UCB, 2019). In 2020, the continued generic erosion in the US has been compensated by recovery from a local, one-time rebate adjustment in Europe and continued growth in international markets, where in Japan the UCB team took over distribution of E Keppra from their former partner, reporting net sales of € 788 million. The incorporation of levetiracetam in the Brazilian public health care system (Sistema Único de Saúde, SUS) was approved in December of 2017 (Brazil, 2017).

During levetiracetam discovery and development, a structure-activity-based study by Kenda *et al.* (2004) showed that the amide moiety, as well as the C4-aliphatic chain, is essential for its pharmacological activity. Moreover, the asymmetric center should have (*S*) absolute configuration and pyrrolidinone is preferable over piperazine or *N*-aliphatic derivatives. To this end, several synthetic routes to levetiracetam have been described in the literature (Anuradha and Preeti, 2013; Chaudhry *et al.*, 2014; Krasowski and McMillin, 2014; Lyseng-Williamson, 2011a; 2011b; Narczyk *et al.*, 2019; Tucker *et al.*, 2009; Uges and Vecht, 2010). However, many of these are long, require an excess of chemicals and solvents that commonly results in the loss of material and use hazardous reagents. It may also involve extreme temperatures (from -78 to 200 °C), protection/deprotection steps and the need of either chromatographic separation or chemical resolution leading to low-efficiency processes from economic and environmental perspectives.

Nowadays, complementary catalytic alternatives to stoichiometric reagents for chemical transformations, such as chemoenzymatic synthetic strategies, are mature and widely adopted in the industrial manufacturing of fine chemicals and active pharmaceutical ingredients, with the aim of making organic synthesis greener (Bisogno *et al.*, 2017; Hönig *et al.*, 2017; Sheldon and Pereira, 2017; Souza *et al.*, 2017). Commercially, levetiracetam is currently produced via a chemoenzymatic process, where the biocatalytic step corresponds to the kinetic resolution of a racemic 2-pyrrolidinonylnitrile catalyzed by an engineered nitrile hydratase (94% enantiomeric excess [*ee*], 43% yield), followed by enantiomeric enrichment (> 99% *ee*) through recrystallization and recycling of the undesired (*R*)-enantiomer by base-mediated racemization (Fig. 1) (Tucker *et al.*, 2009).

Nitrile hydratases (NHase, EC 4.2.1.84) are metalloproteins that contain either non-heme iron(III) or non-corrin cobalt(III) centers in their active site—or zinc in the case of NHases from *Myrothecium verrucaria*—and catalyze the hydration of nitrile into the corresponding amide, without formation of carboxylic acid as a coproduct. The enzyme consists of α - and β -subunits, with the active site being located at the interface of the two subunits (D'Antona and Morrone, 2010). The metal cofactor is bound to the α -subunit, and although the substrate is linked to this subunit, the individual subunit has no catalytic activity (Nelp *et al.*, 2014). The Fe-type NHase exhibits photoreactivity regulated by nitric oxide (NO), while the Co-type NHase does not. Empirical observations relate preferential substrate affinity of Fe-type NHase for small aliphatic nitriles, while Co-type NHase displays preferential affinity for aromatic nitriles due to the differences in their substrate binding pockets (Miyanaga *et al.*, 2004; van Pelt *et al.*, 2011). Initial studies indicated a low stereoselectivity for NHases, where the stereoselective conversion of a nitrile to the corresponding carboxylic acid was conducted by amidases (EC 3.2.1.4) or nitrilases (EC 3.5.5.1), which are other important enzymes in the pathways of nitrile metabolism in nature (Shen *et al.*, 2012). However, even if a poor stereoselectivity is detected for an NHase, it can be engineered through directed evolution, rational design, or combined approaches to generate enzymes with higher stereoselectivity. In addition, the enantioselectivity can be further improved by medium engineering (Tao *et al.*, 2010). The opportunities, as well as many of the challenges, come together in the hydration of bulky nitriles.

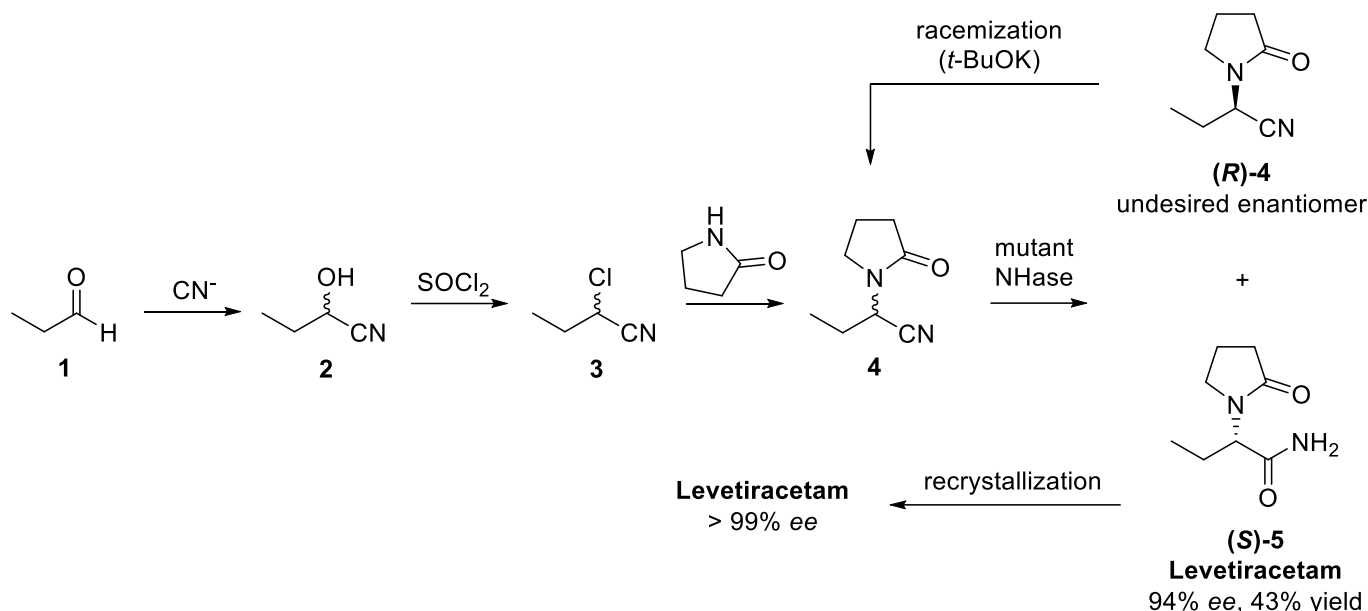


Figure 1. Chemoenzymatic route to levetiracetam using nitrile hydratase (NHase).

Source: Elaborated by the authors using data from [Tucker et al. \(2009\)](#).

In this work, a set of 20 commercially available NHases had their substrate scope and enantioselectivity evaluated towards an ethyl and phenylacetone nitrile series of α -*N*-substituted heterocycles to assess potential biological activities. Initially, the synthetic route used inexpensive aldehydes (propionaldehyde and benzaldehyde) to build α -hydroxynitriles, which had their hydroxyl group substituted by a better leaving group, such as chlorine, with subsequent substitution of chlorine by *N*-heterocycles (2-pyrrolidinone, 2-piperidinone, 2-oxopiperazine and 1-methylpiperazine). However, it was found that the direct *N*-alkylation of these heterocycles could be achieved in high yields directly from the α -hydroxynitriles, thus shortening the route in one step. In addition to the Co-type and Fe-type NHases screening, medium engineering focusing on evaluation of solvent systems to avoid a retro-Strecker reaction in aqueous buffered media, as well as the temperature influence, was investigated. The absolute configuration of α -*N*-heterocyclic ethyl- and phenylacetamides, some of which were new compounds, was determined using electronic circular dichroism (ECD) spectroscopy. Finally, an inhibition assay for acetylcholinesterase was carried out using the freshly prepared α -*N*-heterocyclic ethyl- and phenylacetamides.

2. Experimental

Unless otherwise noted, all reagents and solvents obtained from commercial suppliers were used without

further purification. The 20 nitrile hydratases were obtained from Prozomix Limited ([Prozomix, 2020](#)). Macherey-Nagel Gel 60 F₂₅₄ plates were used for analytical thin layer chromatography (TLC) and visualization under UV light (254 nm) for aromatic compounds or spray reagents (phosphomolybdic acid ethanol solution or *p*-anisaldehyde–sulfuric acid solution) for aliphatic compounds. Dry-column flash chromatography was performed on silica Gel (230–400 mesh) ([Casey et al., 1990](#)). ¹H and ¹³C nuclear magnetic resonance (NMR) spectra were recorded on a Bruker–Fourier 300 operating in 300.19 and 75.48 Hz, respectively, in deuterated chloroform (CDCl₃) or deuterated dimethylsulfoxide (DMSO-*d*₆). ¹⁹F NMR spectra were recorded on a Bruker Avance 400 operating in 376.48 Hz in DMSO-*d*₆. All NMR chemical shifts were expressed in ppm and coupling constants (*J*) in Hertz (Hz), using the solvent signal as internal standard. Fourier transform infrared (FT-IR) were recorded in Thermo Scientific Nicolet iS5 and the scan range was from 4000 to 500 cm⁻¹ in KBr pellet. Melting points (MPs) were measured on a digital device Microquímica MQAPF-302, with a resolution of 0.1 °C in coverslips.

Enzymatic reactions conversions were determined by Shimadzu GC-2010 Plus gas chromatography (GC) equipped with an auto-injector AOC-20i, fitted with a flame ionization detector (FID) and a fused silica capillary column Rtx-5 RESTEK 30 m × 0.25 mm × 0.25 μm. Temperature program: 80 °C (3 min), gradient 30 °C min⁻¹ to 280 °C (5 min). T_{injector} = 260 °C,

$T_{\text{detector}} = 300\text{ }^{\circ}\text{C}$. H_2 was used as carrier gas at a column flow rate of 1.22 mL min^{-1} . Gas chromatography-mass spectrometry analysis (GC-MS) was performed on a Shimadzu GC-2010 plus GC coupled to a Shimadzu MSQP 2010 Plus mass-selective detector in electron ionization (EI, 70 eV) mode. The GC-MS oven was fitted with a fused silica capillary column DB-5 J&W Scientific $30\text{ m} \times 0.25\text{ mm} \times 0.25\text{ }\mu\text{m}$. The same gas chromatography-flame ionization detector (GC-FID) analysis conditions were employed for GC-MS analysis, but with helium as carrier gas.

Enantiomeric excesses (*ees*) were determined by high-performance liquid chromatography (HPLC). Jasco analytical instruments modular HPLC system contained Jasco PU-2089 pump, a Jasco AS-2055 injector, a Jasco MD-2010 diode array detector and a Jasco CD-2095 circular dichroism. Enantiomeric separation of **5a**, **5b** and **9b** were performed using the Chiralcel OD-H column ($250 \times 4.6\text{ mm}$, $5\text{ }\mu\text{m}$, Daicel) in isocratic elution mode with a mixture of *n*-hexane/propan-2-ol 90:10 (v/v) as mobile phase. The enantiomeric separation of **9a** was performed using the Chiralcel IC column ($250 \times 4.6\text{ mm}$, $5\text{ }\mu\text{m}$, Daicel) in isocratic elution with a mixture of hexane/propan-2-ol 70:30 (v/v) as mobile phase. Flow rate was 1.0 mL min^{-1} and circular dichroism operating in 220 nm. Retention times were: (+)-(*R*)-**5a** 18.0 min; (-)-(*S*)-**5a** 24.3 min, (*R*)-**5b** 18.7 min; (*S*)-**5b** 30.0 min, (*R*)-**9a** 31.9 min; (*S*)-**9a** 42.2 min, (*S*)-**9b** 19.8 min; (*R*)-**9b** 24.7 min. The compound (-)-(*S*)-**5a** was confirmed with authentic standard levetiracetam $\geq 98\%$ (Sigma-Aldrich, Saint, Louis, MO, USA) by high-performance liquid chromatography/diode array detector coupled with circular dichroism detection (HPLC-DAD-CD) analysis. The ECD spectra of each enantiomer of **5b**, **9a** and **9b** eluting from the chiral HPLC were measured in the Jasco CD-2095 detector by trapping in a 3.0 cm quartz cell through a switching valve. The spectra were average computed over three instrumental scans, and the intensities are presented in terms of ellipticity values (mdeg). The ECD spectra were baseline corrected by subtraction from a measurement obtained for the same solvent used, as described above.

2.1 General procedure for the synthesis of 2-hydroxybutanenitrile (2)

The aliphatic α -hydroxynitrile **2** was synthesized from propionaldehyde **1** (1 mmol), sodium cyanide (1 mmol) and NaHSO_3 (1 mmol) according to the Young *et al.* (2003) procedure. The crude product was purified by dry-column flash chromatography

(heptane/EtOAc gradient), furnishing **2** as a colorless liquid (70% yield). Infrared (KBr) ν/cm^{-1} 3431, 2976, 2941, 2883, 2248, 1463, 1123, 1104, 1059, 1025, 982; MS (EI 70 eV) m/z (%): 59 (30), 58 (30), 57 (100), 56 (30); ^1H NMR (300.19 MHz, CDCl_3) δ 4.44 (t, 1H, J 6.6 Hz, CH), 1.96–1.80 (m, 2H, CH_2), 1.10 (t, 3H, J 7.4 Hz, CH_3); ^{13}C NMR (75.48 MHz, CDCl_3) δ 119.93 (C_0), 62.48 (CH), 28.49 (CH_2), 8.91 (CH_3).

Caution: all procedures involving sodium cyanide were performed in a well-ventilated lab-hood equipped with a calibrated HCN detector. NeutraliMass spectrometry of HCN-containing waste was performed with commercial bleach (14% sodium hypochlorite solution). The wastes were then stored over a large excess of bleach for disposal.

2.2 Procedure for the synthesis of α -halonitriles (3 and 7)

Based on Choi *et al.* (2016), 0.335 mg of phosphoryl bromide (1.17 mmol) was weighed in a round bottom flask and closed with a rubber septum. With a glass syringe, 450 μL of anhydrous benzene, 195 μL of pyridine (2.4 mmol) and 85 mg of **2** (1 mmol) were added. The reaction mixture was stirred at room temperature for 24 h and the solvent was evaporated under reduced pressure. The residue was diluted in 10 mL of EtOAc and the crude mixture was washed with water ($3 \times 10\text{ mL}$). The organic phase was dried over anhydrous MgSO_4 and the solvent was evaporated, furnishing **3** as a purple liquid (15% yield). Mass spectrometry analysis (EI 70 eV) m/z (%): 121 (12), 119 (12), 81 (13), 79 (13), 68 (83), 52 (16), 41 (100), 39 (57).

The 2-chloro-2-phenylacetonitrile **7** was synthesized from mandelonitrile **6** (1 mmol), pyridine (1.1 mmol) and SOCl_2 (1.1 mmol) in chloroform, according to the Zhang *et al.* (2013) procedure. The crude product was purified by dry-column flash chromatography (hexane/EtOAc gradient), furnishing **7** as a yellow oil (63% yield). Mass spectrometry analysis (EI 70 eV) m/z (%): 59 (30), 58 (30), 57 (100), 56 (30); ^1H NMR (300.19 MHz, CDCl_3) δ 7.58–7.53 (m, 2H, Ar-H), 7.48–7.45 (m, 3H, Ar-H), 5.56 (s, 1H, CH).

2.3 General procedure for the synthesis of α -substituted *N*-heterocyclic nitriles (4a–b and 8a–b)

The reactions were carried out using Teflon-lined stainless-steel autoclave and equipped with a magnetic stirrer, based on the method described by Jenner (1989).

In a typical experiment, $\text{RuCl}_3 \cdot x\text{H}_2\text{O}$ (3.5 mol%) dissolved in 1 mmol of α -hydroxynitrile (2-hydroxybutanenitrile **2** or mandelonitrile **6**) and 5 mmol of nucleophile 2-pyrrolidinone **a** or 2-piperidinone **b** were introduced into the polytetrafluoroethylene (PTFE)-lined stainless steel synthesis autoclave. The autoclave was closed and heated up to 150 °C for 12 h with magnetic stirring and endogenous pressure. The reaction mixture was cooled down to room temperature followed by addition of 5 mL of EtOAc, filtration through filter paper and washing with water basified with NaOH at pH 10 (2×3 mL). The organic phase was dried over anhydrous MgSO_4 and the solvent was evaporated under reduced pressure to give a crude mixture (brown oil), which was purified by dry-column flash chromatography (heptane/EtOAc gradient).

2-(2-oxopyrrolidin-1-yl)butanenitrile (**4a**): orange oil, 38% yield. Purification by dry silica chromatography, 100% EtOAc, IR (KBr) ν/cm^{-1} 3515, 2976, 2938, 2881, 2243, 1690, 1417, 1281, 1216, 933, 814, 642, 567; MS (EI 70 eV) m/z (%): 152 (M^+), 124 (21), 123(100), 112 (37), 84 (17), 69 (66), 68 (35), 41 (50); ^1H NMR (300.19 MHz, CDCl_3) δ 5.01 (t, 1H, J 8.1 Hz, CH), 3.58–3.36 (m, 2H, CH_2^*), 2.43 (t, 2H, J 8.0 Hz, CH_2^*), 2.23–2.00 (m, 2H, CH_2^*), 2.00–1.84 (m, 1H, CH_2), 1.84–1.67 (m, 1H, CH_2), 1.03 (t, 3H, J 7.4 Hz, CH_3); ^{13}C NMR (75.48 MHz, CDCl_3) δ 174.88 (C_0^*), 117.12 (C_0), 44.32 (CH), 43.56 (CH_2^*), 30.47 (CH_2^*), 24.97 (CH_2^*), 17.92 (CH_2), 10.23 (CH_3); *2-oxopyrrolidin-1-yl hydrogens and carbons.

2-(2-oxopiperidin-1-yl)butanenitrile (**4b**): orange oil, 39% yield. Purification by dry silica chromatography, heptane/EtOAc 1:9, IR (KBr) ν/cm^{-1} 3527, 2936, 2878, 2240, 1651, 1487, 1348, 1289, 1178, 1069, 980, 930, 554; MS (EI 70 eV) m/z (%): 166 (M^+), 151 (35), 138 (32), 137 (36), 109 (100), 99 (72), 98 (79), 82 (34), 67 (32), 55 (75), 41 (39); ^1H NMR (300.19 MHz, CDCl_3) δ 5.67 (t, 1H, J 8.2 Hz, CH), 3.54–3.52 (m, 1H, CH_2^*), 3.35–3.25 (m, 1H, CH_2^*), 2.46 (t, 2H, J 6.5 Hz, CH_2^*), 1.93–1.70 (m, 6H, 2CH_2^* and CH_2), 1.03 (t, 3H, J 7.4 Hz, CH_3); ^{13}C NMR (75.48 MHz, CDCl_3) δ 169.87 (C_0^*), 117.77 (C_0), 46.04 (CH), 43.98 (CH_2^*), 32.31 (CH_2^*), 24.25 (CH_2^*), 23.04 (CH_2), 21.05 (CH_2^*), 10.20 (CH_3); *2-oxopiperidin-1-yl hydrogens and carbons.

2-(2-oxopyrrolidin-1-yl)-2-phenylacetonitrile (**8a**): brown oil, 42% yield. Purification by dry silica chromatography, heptane/EtOAc 2:8, IR (KBr) ν/cm^{-1} 3426, 2923, 2243, 1687, 1493, 1455, 1411 1263, 947, 743, 701; MS (EI 70 eV) m/z (%): 200 (M^+), 145 (51), 144 (57), 117 (74), 116 (64), 104 (25), 89 (34), 77 (11); ^1H NMR (300.19 MHz, CDCl_3) δ 7.46–7.38 (m, 5H, Ar-H), 6.47 (s, 1H, CH), 3.56–3.44 (m, 1H, CH_2^*),

3.14–3.04 (m, 1H, CH_2^*), 2.58–2.36 (m, 2H, CH_2^*), 2.20–1.91 (m, 2H, CH_2^*); ^{13}C NMR (75.48 MHz, CDCl_3) δ 174.69 (C_0^*), 131.67 (C_0 , Ar-C), 129.54 (Ar-CH, 3C), 127.27 (Ar-CH, 2C), 115.75 (C_0 , CN), 46.66 (CH), 43.23 (CH_2^*), 30.40 (CH_2^*), 17.65 (CH_2^*); *2-oxopyrrolidin-1-yl hydrogens and carbons.

2-(2-oxopiperidin-1-yl)-2-phenylacetonitrile (**8b**): brown oil, 45% yield. Purification by dry silica chromatography, heptane/EtOAc 3:7, IR (KBr) ν/cm^{-1} 3520, 2939, 2244, 1641, 1485, 1273, 1171, 1076, 981, 921, 821, 725, 695, 651, 544; MS (EI 70 eV) m/z (%): 214 (M^+), 170 (47), 158 (46), 116 (61), 104 (29), 89 (33), 55 (43); ^1H NMR (300.19 MHz, CDCl_3) δ 7.50–7.32 (m, 5H, Ar-H), 7.21 (s, 1H, CH), 3.48–3.36 (m, 1H, CH_2^*), 3.03–2.90 (m, 1H, CH_2^*), 2.64–2.42 (m, 2H, CH_2^*), 1.92–1.72 (m, 4H, CH_2^*); ^{13}C NMR (75.48 MHz, CDCl_3) δ 169.93 (C_0^*), 132.04 (C_0 , Ar-C), 129.36 (Ar-CH, 3C), 127.38 (Ar-CH, 2C), 116.30 (C_0 , CN), 47.99 (CH), 43.81 (CH_2^*), 32.46 (CH_2^*), 22.99 (CH_2^*), 21.12 (CH_2^*); *2-oxopiperidin-1-yl hydrogens and carbons.

2.4 General procedure for the synthesis of α -substituted *N*-heterocyclic nitriles (4c–d and 8c–d)

Based on [Altenkämper et al. \(2009\)](#), 1 mmol of 2-hydroxybutanenitrile **2** or mandelonitrile **6** was dissolved in 0.5 mL acetonitrile (HPLC grade) and 3 mmol of 2-oxopiperazine **c** or 1-methylpiperazine **d** were added. The mixture was heated under reflux for 5–8 h (for reactions with 2-hydroxybutanenitrile) and 20–24 h (for reactions with mandelonitrile). After removing the acetonitrile under reduced pressure, 5 mL EtOAc was added, and the crude mixture was washed with a saturated solution of K_2CO_3 (3×3 mL). The organic phase was dried over anhydrous MgSO_4 , and the solvent was evaporated to yield the expected product.

2-(3-oxopiperazin-1-yl)butanenitrile (**4c**): white solid, 20% yield. Melting point 114–115 °C; IR (KBr) ν/cm^{-1} 3266, 2975, 2940, 2883, 2798, 2227, 1664, 1347, 1170, 1077, 855, 753, 622; MS (EI 70 eV) m/z (%): 167 (M^+), 138 (98), 110 (100), 99 (31), 97 (27), 42 (82), 41 (35); ^1H NMR (300.19 MHz, CDCl_3) δ 6.37 (bs, 1H, NH), 3.56–3.12 (m, 5H, CH and 2CH_2^*), 2.96–2.84 (m, 1H, CH_2^*), 2.75–2.58 (m, 1H, CH_2^*), 1.94–1.75 (m, 2H, CH_2), 1.08 (t, 3H, J 7.4 Hz, CH_3); ^{13}C NMR (75.48 MHz, CDCl_3) δ 168.31 (C_0^*), 116.21 (C_0 , CN), 58.76 (CH), 53.28 (CH_2^*), 46.39 (CH_2^*), 41.18 (CH_2^*), 24.43 (CH_2), 10.64 (CH_3); *3-oxopiperazin-1-yl hydrogens and carbons.

2-(4-methylpiperazin-1-yl)butanenitrile (**4d**): yellow oil, 38% yield. Infrared (KBr) ν/cm^{-1} 2937, 2878, 2797, 2222, 1456, 1377, 1285, 1167, 1010, 859, 809; MS (EI 70 eV) m/z (%): 167 (M^+), 141 (3), 140 (4), 111 (13), 99 (100), 70 (31), 56 (66); ^1H NMR (300.19 MHz, CDCl_3) δ 3.39 (dd, 1H, J 8.6, 7.1 Hz, CH), 2.82–2.67 (m, 2H, CH_2^*), 2.64–2.40 (m, 6H, CH_2^*), 2.32 (s, 3H, CH_3^*), 1.91–1.66 (m, 2H, CH_2), 1.06 (t, 3H, J 7.4 Hz, CH_3); ^{13}C NMR (75.48 MHz, CDCl_3) δ 117.02 (C_0), 59.55 (CH), 54.82 (CH_2^* , 4C), 45.85 (CH_3^*), 24.47 (CH_2), 10.76 (CH_3); *4-methylpiperazin-1-yl hydrogens and carbons.

2-(3-oxopiperazin-1-yl)-2-phenylacetoneitrile (**8c**): white solid, 22% yield. Melting point 173–175 °C; IR (KBr) ν/cm^{-1} 3439, 3208, 2972, 2893, 2849, 2231, 1666, 1497, 1334, 1156, 1069, 758, 710, 521; MS (EI 70 eV) m/z (%): 215 (M^+), 186 (7), 171 (9), 145 (16), 116 (73), 99 (100), 89 (25), 43 (29), 42 (64); ^1H NMR (300.19 MHz, $\text{DMSO}-d_6$) δ 7.91 (s, 1H, NH), 7.51–7.39 (m, 5H, Ar-H), 5.52 (s, 1H, CH), 3.26–3.05 (m, 3H, CH_2^*), 2.85 (d, 1H, J 15.9 Hz, CH_2^*), 2.74–2.62 (m, 1H, CH_2^*), 2.62–2.53 (m, 1H, CH_2^*); ^{13}C NMR (75.48 MHz, $\text{DMSO}-d_6$) δ 166.42 (C_0^*), 132.54 (C_0 , Ar-C), 128.96 (Ar-CH, 3C), 127.75 (Ar-CH, 2C), 115.48 (C_0 , CN), 59.57 (CH), 53.16 (CH_2^*), 45.42 (CH_2^*), 40.02 (CH_2^*); *3-oxopiperazin-1-yl hydrogens and carbons.

2-(4-methylpiperazin-1-yl)-2-phenylacetoneitrile (**8d**): yellow solid, 71% yield. Melting point 63–64 °C; IR (KBr) ν/cm^{-1} 3442, 3064, 2946, 2827, 2792, 2223, 1450, 1285, 1144, 1010, 914, 812, 736, 700; MS (EI 70 eV) m/z (%): 215 (M^+), 116 (10), 99 (100), 70 (19), 56 (60), 44 (37), 42 (26); HRMS (ESI) m/z , observed: 216.1489; $\text{C}_{13}\text{H}_{17}\text{N}_3$ [$M+\text{H}$] $^+$ requires: 216.1495; ^1H NMR (300.19 MHz, CDCl_3) δ 7.56–7.47 (m, 2H, Ar-H), 7.45–7.33 (m, 3H, Ar-H), 4.82 (s, 1H, CH), 2.63 (m, 4H, CH_2^*), 2.47 (m, 4H, CH_2^*), 2.31 (s, 3H, CH_3^*); ^{13}C NMR (75.48 MHz, CDCl_3) δ 133.10 (C_0 , Ar-C), 129.01 (Ar-CH, 3C), 128.09 (Ar-CH, 2C), 115.45 (C_0 , CN), 62.14 (CH), 54.87 (CH_2^* , 4C), 45.89 (CH_3^*); *4-methylpiperazin-1-yl hydrogens and carbons.

2.5 General procedure for the synthesis of racemic amides (5a–b, 5d, 9a–b and 9d)

Based on González-Vera *et al.* (2005), 1 mmol of the corresponding α -substituted *N*-heterocyclic nitriles (**4a–b**, **4d** and **8a–b** and **8d**) were dissolved in 4 mL CH_2Cl_2 and followed by addition of 1.7 mL concentrated H_2SO_4 . The mixture was stirred at room temperature (at different reaction times according to each compound, as shown below). After that, the reaction mixture was taken to an ice bath, neutralized

with NaOH and extracted with EtOAc (3×10 mL). The organic phases were combined, dried over anhydrous MgSO_4 and the solvent was evaporated under vacuum. Further purification was not necessary.

2-(2-oxopyrrolidin-1-yl)butanamide (**5a**): reaction time 4 h, white solid, 80% yield. Melting point 116–117 °C; IR (KBr) ν/cm^{-1} 3392, 3320, 3255, 3204, 2966, 2922, 2871, 1677, 1271, 1442, 694, 629; MS (EI 70 eV) m/z (%): 170 (M^+), 126 (100), 98 (12), 69 (28), 58 (13), 41 (26); ^1H NMR (300.19 MHz, CDCl_3) δ 6.33 (bs, 1H, CONH_2), 5.46 (bs, 1H, CONH_2), 4.45 (dd, 1H, J 8.8, 6.9 Hz, CH), 3.49–3.35 (m, 2H, CH_2^*), 2.54–2.35 (m, 2H, CH_2^*), 2.12–1.89 (m, 3H, CH_2^* and CH_2), 1.78–1.61 (m, 1H, CH_2), 0.91 (t, 3H, J 7.4 Hz, CH_3); ^{13}C NMR (75.48 MHz, CDCl_3) δ 176.26 (C_0^*), 172.41 (C_0), 56.30 (CH), 44.07 (CH_2^*), 31.20 (CH_2^*), 21.15 (CH_2^*), 18.28 (CH_2), 10.62 (CH_3); *2-oxopyrrolidin-1-yl hydrogens and carbons.

2-(2-oxopiperidin-1-yl)butanamide (**5b**): reaction time 60 h, brown solid, 21% yield. Melting point 106–108 °C; IR (KBr) ν/cm^{-1} 3351, 3204, 2947, 2872, 1675, 1626, 1465, 1419, 1288, 1181, 976, 668; MS (EI 70 eV) m/z (%): 184 (M^+), 167 (7), 141 (10), 140 (100), 112 (25), 70 (12), 55 (24), 41 (13); ^1H NMR (300.19 MHz, CDCl_3) δ 6.33 (bs, 1H, CONH_2), 5.33 (bs, 1H, CONH_2), 5.00 (dd, 1H, J 8.5, 7.3 Hz, CH), 3.32–3.17 (m, 2H, CH_2^*), 2.59–2.30 (m, 2H, CH_2^*), 2.00–1.65 (m, 6H, 2CH_2^* and CH_2), 0.91 (t, 3H, J 7.4 Hz, CH_3); ^{13}C NMR (75.48 MHz, CDCl_3) δ 172.74 (C_0^*), 171.48 (C_0), 57.37 (CH), 43.40 (CH_2^*), 32.64 (CH_2^*), 23.25 (CH_2^*), 20.94 (CH_2^*), 20.13 (CH_2), 10.58 (CH_3); *2-oxopiperidin-1-yl hydrogens and carbons.

2-(4-methylpiperazin-1-yl)butanamide (**5d**): Reaction time 22 h, orange oil, 28% yield. Infrared (KBr) ν/cm^{-1} 3357, 2962, 2798, 1671, 1459, 1284, 1172, 1010, 866, 640; MS (EI 70 eV) m/z (%): 185 (M^+), 142 (10), 141 (100), 98 (50), 70 (65), 56 (21), 42 (29); ^1H NMR (300.19 MHz, CDCl_3) δ 6.77 (bs, 1H, CONH_2), 5.57 (bs, 1H, CONH_2), 2.82 (dd, 1H, J 7.4, 5.2, CH), 2.76–2.48 (m, 8H, 4CH_2^*), 2.36 (s, 3H, CH_3^*), 1.83–1.65 (m, 2H, CH_2), 0.99 (t, J 7.5, CH_3); ^{13}C NMR (75.48 MHz, CDCl_3) δ 175.86 (C_0), 70.62 (CH), 55.48 (4CH_2^*), 45.88 (CH_3^*), 21.56 (CH_2), 11.03 (CH_3); *4-methylpiperazin-1-yl hydrogens and carbons.

2-(2-oxopyrrolidin-1-yl)-2-phenylacetamide (**9a**): reaction time 20 h, white solid, 96% yield. Melting point 156–157 °C; IR (KBr) ν/cm^{-1} 3383, 3314, 3257, 3201, 2964, 2924, 2872, 1674, 1423, 1270, 702, 619, 549; MS (EI 70 eV) m/z (%): 174 (100), 131 (36), 106 (18), 91 (19), 77 (9), 70 (1); ^1H NMR (300.19 MHz, CDCl_3) δ 7.41–7.35 (m, 5H, Ar-H), 5.94 (bs, 1H, CONH_2), 5.89 (s, 1H, CH), 5.75 (bs, 1H, CONH_2), 3.78–3.65 (m, 1H, H-12), 3.10–2.98 (m, 1H, CH_2^*),

2.56–2.30 (m, 2H, CH₂*), 2.09–1.99 (m, 1H, CH₂*), 1.971.82 (m, 1H, CH₂*); ¹³C NMR (75.48 MHz, CDCl₃) δ 175.82 (C₀*), 171.44 (C₀), 134.33 (C₀, Ar-C), 129.30 (Ar-CH, 2C), 129.12 (Ar-CH, 2C), 128.88 (Ar-CH, 1C), 58.74 (CH), 45.02 (CH₂*), 31.08 (CH₂*), 18.19 (CH₂*); *2-oxopyrrolidin-1-yl hydrogens and carbons.

2-(2-oxopiperidin-1-yl)-2-phenylacetamide (**9b**): reaction time 60 h, brown solid, 58% yield. Melting point 154–155 °C; IR (KBr) ν/cm^{-1} 3313, 3161, 2960, 2869, 1697, 1613, 1484, 1412, 1296, 1178, 740, 701, 516; MS (EI 70 eV) m/z (%): 232 (M⁺), 215 (12), 189 (17), 188 (100), 91 (45), 82 (20), 55 (18); ¹H NMR (300.19 MHz, CDCl₃) δ 7.47–7.30 (m, 5H, Ar-H), 6.34 (s, 1H, CH), 5.92 (bs, 1H, CONH₂), 5.64 (bs, 1H, CONH₂), 3.52–3.38 (m, 1H, CH₂*), 2.96–2.84 (m, 1H, CH₂*), 2.60–2.39 (m, 2H, CH₂*), 1.90–1.60 (m, 4H, 2CH₂*); ¹³C NMR (75.48 MHz, CDCl₃) δ 171.70 (C₀*), 171.10 (C₀), 134.52 (C₀, Ar-C), 129.70 (Ar-CH, 2C), 128.96 (Ar-CH, 2C), 128.65 (Ar-CH, 1C), 60.34 (CH), 45.27 (CH₂*), 32.57 (CH₂*), 23.30 (CH₂*), 21.04 (CH₂*); *2-oxopiperidin-1-yl hydrogens and carbons.

2-(4-methylpiperazin-1-yl)-2-phenylacetamide (**9d**): reaction time 23 h, brown solid, 85% yield. Melting point 163–165 °C; IR (KBr) ν/cm^{-1} 3405, 3176, 2949, 2795, 1655, 1449, 1291, 1157, 1011, 854, 692, 663; MS (EI 70 eV) m/z (%): 233 (M⁺), 190 (14), 189 (100), 146 (13), 91 (37), 70 (35), 56 (16), 42 (22); ¹H NMR (300.19 MHz, CDCl₃) δ 7.39–7.28 (m, 5H, Ar-H), 6.85 (bs, 1H, CONH₂), 5.62 (bs, 1H, CONH₂), 3.86 (s, 1H, CH), 2.57 (m, 8H, 4CH₂*), 2.35 (s, 3H, CH₃*); ¹³C NMR (75.48 MHz, CDCl₃) δ 174.02 (C₀), 135.55 (C₀, Ar-C), 128.94 (Ar-CH, 2C), 128.85 (Ar-CH, 2C), 128.59 (Ar-CH, 1C), 75.75 (CH), 55.10 (4CH₂*), 45.54 (CH₃*); *4-methylpiperazin-1-yl hydrogens and carbons.

2.6 Enzymatic activity assay

Five microliters of NHases were suspended in 1 mL of Na-phosphate buffer (0.1 mol L⁻¹, pH 7.00) in an Eppendorf tube followed by addition of *n*-butanenitrile (1 mg, 14.5 μmol). The reaction was allowed to proceed for 1 min at 25 °C and 1000 rpm. After this period, the reaction was interrupted by the addition of 500 μL of EtOAc and the organic phase was analyzed by GC-FID. The enzymatic activity was measured by monitoring the *n*-butanenitrile consumption through the analytical curve ($y = 20972x + 7121.9$, $R^2 = 0.990$). All enzymatic assays were performed in Na-phosphate buffer enriched with 0.8 μg L⁻¹ of CoCl₃·6H₂O and 0.8 μg L⁻¹ FeCl₃·6H₂O. Before performing the enzymatic assays

with Fe-type NHases, the enzymes were light reactivated by incubating them in Na-phosphate buffer (0.1 mol L⁻¹, pH 7.0) on ice bath under sunlight for 1.5 h.

2.7 General procedure for NHase-catalyzed synthesis of amides in buffered aqueous medium

In an Eppendorf tube, 1 mL of Na-phosphate buffer (0.1 mol L⁻¹, pH 7.00), 10 μL of NHases, and 5 μmol of substrate (**4a–d** and **8a–d**) were added. The reactions were allowed to proceed for 48 h at 25 °C and 1000 rpm. After that, 500 μL EtOAc was added and the mixture vortexed and centrifuged at 5000 rpm for 1 min. The organic phase was analyzed by GC-FID to determine the conversion rates. Enantiomeric excesses were determined by HPLC-DAD-CD (EtOAc was eliminated under mild heating, 35 °C, and samples were dissolved in propan-2-ol). Control assays were carried out under the same experimental conditions; however, in the absence of the NHases.

2.8 General procedure for ionic liquids synthesis

Ionic liquids have been synthesized in two steps. Firstly 1-butyl-3-methylimidazolium chloride (BMIM.Cl) was prepared. Then, a metathesis reaction between the salt containing the corresponding anion and an alkali metal cation gave the ionic liquid (IL) of interest.

2.8.1 Synthesis of 1-butyl-3-methylimidazolium chloride

N-methylimidazole and 1-chlorobutane were refluxed in acetonitrile following the same procedure described by Dupont *et al.* (2002) furnishing BMIM.Cl. The white solid highly hygroscopic was obtained in 88% yield and stored under N₂. ¹H NMR (300.19 MHz, DMSO-*d*₆) δ 9.14 (s, 1H, CH*), 7.73 (dt, 2H, *J* 20.3, 1.7 Hz, CH*), 4.15 (t, 2H, *J* 7.2 Hz, CH₂), 3.84 (s, 3H, CH₃*), 1.84–1.67 (m, 2H, CH₂), 1.33–1.13 (m, 2H, CH₂), 0.90 (t, 3H, *J* 7.3 Hz, CH₃); ¹³C NMR (75.48 MHz, DMSO-*d*₆) δ 136.70 (CH*), 123.60 (CH*), 122.28 (CH*), 48.42 (CH₂), 35.73 (CH₃*), 31.39 (CH₂), 18.78 (CH₂), 13.30 (CH₃); *3-methylimidazolium hydrogens and carbons.

2.8.2 General procedure for the synthesis of the ionic liquids of interest

An equimolar mixture of salt (NaBF₄, KPF₆ or LiNTf₂) and BMIM.Cl was vigorously stirred at room temperature for 24 h in excess of acetone. The reaction mixture was filtered in celite column and concentrated under reduced pressure and mild heating (30 °C). The obtained viscous liquid was dissolved in CH₂Cl₂ and washed with water (3×). The organic phase was dried over anhydrous MgSO₄ under stirring for 1 h, followed by solvent evaporation under reduced pressure giving the IL.

1-butyl-3-methylimidazolium tetrafluoroborate (BMIM.BF₄): ¹H NMR (300.19 MHz, DMSO-*d*₆) δ 9.06 (s, 1H, CH*), 7.74 (t, 1H, *J* 1.8 Hz, CH*), 7.67 (t, 1H, *J* 1.7 Hz, CH*), 4.13 (t, 2H, *J* 7.2 Hz, CH₂), 3.82 (s, 3H, CH₃*), 1.82–1.67 (m, 2H, CH₂), 1.23 (dq, 2H, *J* 14.5, 7.3 Hz, CH₂), 0.88 (t, 3H, *J* 7.3 Hz, CH₃); ¹³C NMR (75.48 MHz, DMSO-*d*₆) δ 136.51 (CH*), 123.65 (CH*), 122.30 (CH*), 48.54 (CH₂), 35.76 (CH₃*), 31.38 (CH₂), 18.81 (CH₂), 13.30 (CH₃). ¹⁹F NMR (376.48 MHz, DMSO-*d*₆) δ -148.29, -148.34; DSC -67 °C (T_g, crystallization temperature) and -74 °C (T_m, melting temperature); *3-methylimidazolium hydrogens and carbons.

1-butyl-3-methylimidazolium hexafluorophosphate (BMIM.PF₆): ¹H NMR (300.19 MHz, DMSO-*d*₆) δ 9.07 (s, 1H, CH*), 7.74 (t, 1H, *J* 1.8 Hz, CH*), 7.67 (t, 1H, *J* 1.7 Hz, CH*), 4.13 (t, 2H, *J* 7.2 Hz, CH₂), 3.82 (s, 3H, CH₃*), 1.84–1.63 (m, 2H, CH₂), 1.23 (m, 2H, CH₂), 0.88 (t, 3H, *J* 7.3 Hz, CH₃); ¹³C NMR (75.48 MHz, DMSO-*d*₆) δ 136.52 (CH*), 123.65 (CH*), 122.29 (CH*), 48.54 (CH₂), 35.76 (CH₃*), 31.37 (CH₂), 18.80 (CH₂), 13.29 (CH₃). ¹⁹F NMR (376.48 MHz, DMSO-*d*₆) δ -70.20 (d, *J* 711.4 Hz); DSC -64 °C (T_g) and 6 °C (T_m); *3-methylimidazolium hydrogens and carbons.

1-butyl-3-methylimidazolium bis(trifluoromethylsulfonyl)imide (BMIM.NTf₂): ¹H NMR (300.19 MHz, DMSO-*d*₆) δ 9.07 (s, 1H, CH*), 7.74 (t, 1H, *J* 1.8 Hz, CH*), 7.67 (t, 1H, *J* 1.7 Hz, CH*), 4.13 (t, 2H, *J* 7.2 Hz, CH₂), 3.82 (s, 3H, CH₃*), 1.81–1.66 (m, 2H, CH₂), 1.32–1.15 (m, 2H, CH₂), 0.88 (t, 3H, *J* 7.3 Hz, CH₃); ¹³C NMR (75.48 MHz, DMSO-*d*₆) δ 136.53 (CH*), 123.65 (CH*), 122.30 (CF₃), 121.65 (CH*), 117.36 (CF₃), 48.54 (CH₂), 35.77 (CH₃*), 31.38 (CH₂), 18.80 (CH₂), 13.29 (CH₃); ¹⁹F NMR (376.48 MHz, DMSO-*d*₆) δ -78.73 (s); DSC -85 °C (T_g) and -2.5 °C (T_m); *3-methylimidazolium hydrogens and carbons.

2.9 General procedure for NHase-catalyzed synthesis of amides in nonconventional media

The reactions were carried out under monophasic system (buffer: PEG400 and BMIM.BF₄) or biphasic system (buffer: BMIM.PF₆ and BMIM.NTf₂). The final volume of all reactions was 1 mL. The ratios of buffer: ionic liquids were 10, 20, 40 and 80% (v/v) and buffer PEG400 were 10, 25, 50, 95 and 100% (v/v).

In an Eppendorf tube 1 mL of buffer: nonconventional media solution was added, followed by 10 μL of PRO-NHASE(001) or PRO-NHASE(015) and 5 μmol of substrate (**4a–d** and **8a–d**). The reactions were allowed to proceed for 48 h at 25 °C and 1500 rpm. After that 500 μL of Et₂O was added to BMIM.BF₄, BMIM.PF₆ and PEG400 reactions, and 500 μL EtOAc to BMIM.NTf₂ reactions. The mixture was vortexed and centrifuged at 5000 rpm for 1 min. The organic phase was analyzed by GC-FID for conversion measurements.

2.10 Electronic circular dichroism calculations

All density functional theory (DFT) and time-dependent-DFT (TDDFT) calculations were carried out at 298 K in the gas phase with the Gaussian 09 (2016) software. Calculations were performed for the arbitrarily chosen *S*-configuration for **5b** and **9a–9b**. The conformational searches were carried out at the molecular mechanics level of theory with the Monte Carlo algorithm employing the MM+ force field, incorporated in HyperChem 8.0.10 software. Initially, for compound (*S*)-**5b**, ten conformers with a relative energy (rel E.) within 6 kcal mol⁻¹ were selected and geometry optimized at the B3LYP/6-31G(d) level. The six conformers with rel E. < 1.8 kcal mol⁻¹ were selected for UV and ECD spectral calculations. Regarding (*S*)-**9a** and (*S*)-**9b**, the conformational searches resulted in six conformers for both compounds, with rel E. within 6 kcal mol⁻¹, which were geometry optimized at the B3LYP/6-31G(d) level. The four and two conformers, respectively, with rel E. < 2.0 kcal mol⁻¹ were selected for UV and ECD spectral calculations. Vibrational analysis at the B3LYP/6-31G(d) level resulted in no imaginary frequencies for all conformers, confirming them as real minima. The TDDFT was employed to calculate the excitation energy (in nm) and rotatory strength *R* in the dipole velocity (*R*_{vel} in cgs units: 10⁻⁴⁰ esu² cm²) form, at the CAM-B3LYP/TZVP level. The calculated rotatory strengths from the first 30 singlet → singlet electronic transitions were simulated into an ECD curve using

Gaussian bands with a bandwidth of σ 0.25 eV. The predicted wavelength transitions were multiplied with a scaling factor of 0.99, determined by the best agreement between experimental and calculated UV spectra. The Boltzmann factor for each conformer was calculated based on Gibbs free energies.

2.11 Cholinesterase inhibition screening assays

The *N*-heterocycles compounds (**5a**, **5b**, **9a** and **9b**) were submitted to cholinesterases inhibition screening assay using the simultaneous on-flow dual parallel enzyme assay system (Seidl *et al.*, 2019). Acetylcholinesterase from *Electrophorus electricus* (eeAChE) and butyrylcholinesterase from *human serum* (BChE) were immobilized independently onto fused silica capillary (0.1 mm I.D \times 0.375 mm \times 30 cm), as previously described elsewhere (Vilela *et al.*, 2018), formed the capillary bioreactors AChE-ICER) and BChE-ICER, where ICER means immobilized capillary enzyme reactor.

The on-flow dual parallel enzyme assay was carried out on a LC system (Nexera Shimadzu) consisting of three LC 20AD pumps, a SIL-20A auto-sampler, a DGU-20A degasser, a CTO-20A oven, and a CBM-20A system controller. The LC system was coupled with an AmaZon speed ion trap (IT) mass spectrometry (MS) instrument (Bruker Daltonics) equipped with an electrospray ionization (ESI) interface source, operating in a positive mode (scan m/z 50–250).

The two ICER and the MS instrument were interfaced through two 10-port two-position high-pressure switching valves (Valco Instruments Co. Inc.) (Seidl *et al.*, 2019).

The dual system assay consisted of three steps. Briefly, after sample injection, valves (A and B) in position 1, the reactive content of each ICER was transferred to the storage (step 1). In step 2, with both valves (A and B) in position 2, pump B directed the enzymatic reaction of eeAChE-ICER for analysis in the MS. Meanwhile, the reactive content of huBChE-ICER was held in storage. In step 3, while valve A was switched to position 1 again, valve B was kept in position 2. In this position, the huBChE-ICER enzymatic reaction content held in storage was flushed by pump B and finally analyzed in the MS. Detailed system configuration description, MS parameters, assay inhibition are described in Seidl *et al.* (2019).

Data acquisition was carried out using the Bruker Data Analysis Software (version 4.3). All analyses were performed at room temperature (21 °C). The enzymatic reaction was monitored by direct quantification of

acetylcholine hydrolysis product, choline (Ch) $[M + H]^+$ m/z 104 (Seidl *et al.*, 2019; Vilela *et al.*, 2018).

N-heterocycles samples were solubilized in methanol to a stock solution of 1.00 mmol L⁻¹ for each compound. Tacrine was used as standard cholinesterase inhibitor.

The assay inhibition was prepared with 10 μ L of each stock solution (100 μ mol L⁻¹ final concentration), 20 μ L of acetylcholine (ACh) solution (70 μ mol L⁻¹ final concentration) and 70 μ L of ammonium acetate solution (15.0 mmol L⁻¹, pH 8.0). Solutions were prepared in duplicate and 20 μ L aliquots were used for injection. Negative (absence of ACh) and positive (presence of ACh and absence of ligand) controls were analyzed between each sample. Percentage inhibition displayed by each sample was calculated by comparison between the area of enzymatic activity in the presence of the inhibitor (P_i) and absence (P_0), according to the following Eq. 1:

$$\% \text{ inhibition} = \left[1 - \left(\frac{P_i - S_b}{P_0 - S_b} \right) \right] \times 100 \quad (1)$$

where P is the attained peak area of Ch produced: (P_i) in the presence of the tested compound; (P_0) in the absence of the tested compound, and S_b is Ch quantified during spontaneous ACh hydrolysis. S_b was determined by injecting the reaction mixture into an empty open tubular silica capillary (blank analysis to quantify spontaneous ACh hydrolysis).

3. Results and discussion

3.1 Synthesis of α -substituted *N*-heterocyclic nitriles

The first proposed retrosynthetic analysis of the target α -substituted *N*-heterocyclic nitriles (**4a–d** and **8a–d**) is outlined in Fig. 2. However, it was found that **4a–d** and **8a–d** could be obtained directly from the corresponding α -hydroxynitriles (**2** and **6**) via *N*-alkylation.

Whereas α -hydroxynitrile **6** is inexpensive and commercially available, the α -hydroxynitrile **2** was readily prepared from propanaldehyde **1** and a cyanide donor. Aiming at a safer and greener cyanide donor for the synthesis of **2**, the reaction proposed by Wen *et al.* (2012) was evaluated, which uses trimethylsilyl cyanide (TMSCN) and a quaternary ammonium as a phase transfer catalyst. However, the obtained yield of 49% was not sufficient for the first synthetic step (data not shown). Thus, the classical approach by addition of

sodium cyanide in the presence of sodium bisulfite was used, with yield of 70% for **2** (Young *et al.*, 2003).

It is well known that hydroxyl group is a poor leaving group (LG) and is usually replaced by a better one, such as tosyl, mesyl, or halogens. However, in order to avoid a functional group manipulation step, a direct alkylation of the following *N*-heterocycles was

attempted: **a**, 2-pyrrolidinone; **b**, 2-piperidinone; **c**, 2-oxopiperazine; and **d**, 1-methylpiperazine with α -hydroxynitriles (Altenkämper *et al.*, 2009; Jenner, 1989). The results are shown in Tab. 1. The main advantages of the direct *N*-alkylation strategy are the reduction in the number of reaction steps and the generation of fewer residues.

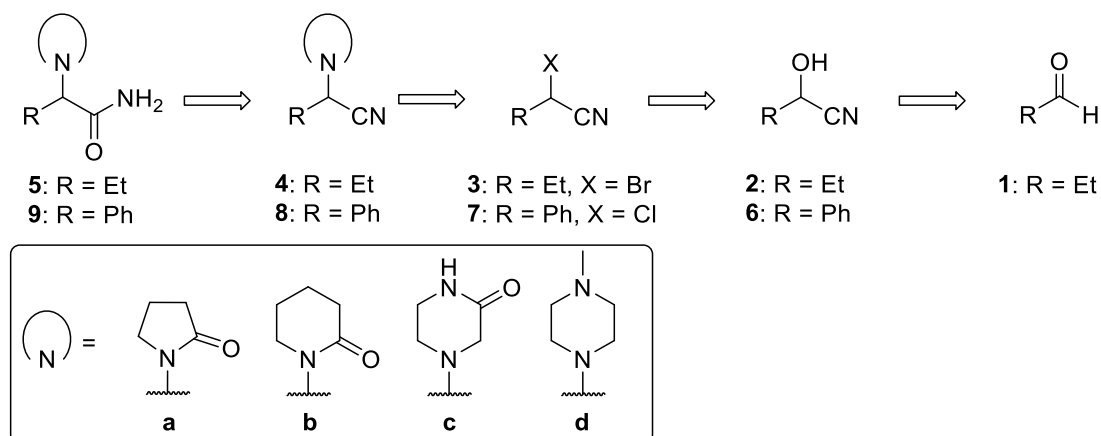


Figure 2. Retrosynthetic route to α -substituted *N*-heterocyclic amides.

Table 1. *N*-heterocyclic alkylation with α -hydroxynitrile and α -halonitrile.

Entry	α -Substituted nitrile	<i>N</i> -heterocycle	Product	Reaction time (h)	Yield (%) ^c
1	2	a , 2-pyrrolidinone ^a	4a	12	50
2	2	b , 2-piperidinone ^a	4b	12	52
3	2	c , 2-oxopiperazine ^b	4c	12	40
4	2	d , 1-methylpiperazine ^b	4d	12	60
5	6	a , 2-pyrrolidinone ^a	8a	12	42
6	6	b , 2-piperidinone ^a	8b	12	48
7	6	c , 2-oxopiperazine ^b	8c	12	35
8	6	d , 1-methylpiperazine ^b	8d	12	71
9	3	d , 1-methylpiperazine ^b	4d	10	59
10	7	c , 2-oxopiperazine ^b	8c	24	27
11	7	d , 1-methylpiperazine ^b	8d	20	75

^aGeneral conditions: α -hydroxynitrile (1 mmol), *N*-heterocycle (5 mmol) and $\text{RuCl}_3 \cdot x\text{H}_2\text{O}$ (3.5 mol%) at 150 °C (autoclave);

^bgeneral conditions: α -hydroxynitriles (1 mmol, 0.5 mL ACN solution), *N*-heterocycle (3 mmol) and heating under reflux;

^cisolated yields.

The *N*-alkylation of both piperazine derivatives, 2-oxopiperazine and 1-methylpiperazine, with α -hydroxynitriles **2** and **6**, proceeded smoothly in the presence of acetonitrile (ACN) under reflux, with yields of 35–71%, after 12 h (Tab. 1, entries 3, 4, 7, and 8).

However, under the same conditions no alkylation was observed for 2-pyrrolidinone and 2-piperidinone, and the starting materials were quantitatively recovered after 24 h. These results could be rationalized by the fact that lactams are less basic than amines, as it can be

seen for the heterocycle **c** in which the *N*-alkylation occurred through the amine moiety and not in the amide moiety. Also, reactions with **d** showed better yields than **c**, since the first one is more basic. To circumvent the lack of *N*-alkylation with the lactam heterocycles **a** and **b**, a reaction using RuCl₃ as catalyst in an autoclave was studied. By carrying out the reaction under 3.5 mol% of catalyst load and 150 °C, moderate yields (42–52%, Tab. 1, entries 1, 2, 5, and 6) of the desired products were obtained after 12 h.

To compare the efficiency of *N*-alkylation of α -hydroxynitriles and α -halonitriles, the chlorination of mandelonitrile **6** was performed using thionyl chloride and pyridine as catalyst (Zhang *et al.*, 2013) under reflux and obtained the 2-chloro-2-phenylacetonitrile **7** in 63% yield. The *N*-alkylation of **7** was carried out under the same reaction conditions previously described for the α -hydroxynitriles. Again, in the absence of ruthenium catalyst, the reaction proceeded only for the piperazine derivatives **c** and **d**, with yields in the same range of the ones obtained with the directly *N*-alkylation of **6** (Tab. 1, entries 10 and 11). Even with a better LG, the lactams **a** and **b** nucleophilicity were not sufficient and the ruthenium catalyst was necessary to afford the correspondent pyrrolidinone and piperidinone derivatives, **8a** and **8b**, in moderate yields. The chlorination of aliphatic α -hydroxynitrile **2** failed after

many attempts using thionyl chloride under different reaction conditions. Then, the bromination of **2** was performed with phosphoryl bromide and pyridine as catalyst (Choi *et al.*, 2016) at room temperature and the 2-bromobutanenitrile **3** in 15% yield was obtained. The *N*-alkylation of **3** was carried out only with piperazine **d** due to the low yield in the halogenation step (Tab. 1, entry 9). The comparison between the *N*-alkylation of α -hydroxynitriles and α -halonitriles stress the better performance of the shorter route leading to a better overall yield and generating fewer residues.

With the α -substituted *N*-heterocyclic nitriles successfully synthesized by directly replacement of α -hydroxynitriles, the scope of enzymatic nitrile hydration was then investigated with a series of Fe-type and Co-type nitrile hydratases.

3.2 Synthesis of α -substituted *N*-heterocyclic amides

The racemic amides were synthesized via classical acid catalysis (H₂SO₄) in dichloromethane (González-Vera *et al.*, 2005) and used as standards for the development of chiral chromatographic methods. The results are shown in Tab. 2.

Table 2. Hydration of α -substituted *N*-heterocyclic nitriles to corresponding amides^a.

Entry	α -Substituted nitrile	Product	Reaction time (h)	Yield (%) ^b
1	4a	5a	4	80
2	4b	5b	60	21
3	4c	5c	60	n.r.
4	4d	5d	22	28
5	8a	9a	20	96
6	8b	9b	60	58
7	8c	9c	60	n.r.
8	8d	9d	23	85

^aGeneral conditions: α -substituted *N*-heterocyclic nitriles (1 mmol), dichloromethane (4 mL) and concentrated sulfuric acid (30 equivalents, 1.7 mL) at room temperature and over magnetic agitation; ^bisolated yields; n.r. = no reaction.

In all cases, no further purification step was necessary after extraction of the products. The nitriles **4c** and **8c** did not lead to the formation of the desired products **5c** and **9c**, respectively. Both compounds are

insoluble in the reaction medium and, even when the reactions were carried out in the presence of DMSO as a cosolvent, there was no product formation.

Except for levetiracetam **5a**, to the best of authors knowledge this is the first time that the α -substituted-*N*-heterocyclic amides **5b**, **5d**, **9a**, **9b**, and **9d** have been synthesized and characterized, as well as their respective α -substituted-*N*-heterocyclic nitriles **4b–d**, **8a–d**.

3.3 Enzymatic reactions with NHases

3.3.1 Nitrile hydratase activity

Twenty NHases commercially available from Prozomix Ltd (Prozomix, 2020) were purchased. For characterization, their activities were monitored by GC-

FID using *n*-butanenitrile as a substrate. One unit of enzymatic activity was defined as the amount (μmol) of *n*-butanamide formed from *n*-butanenitrile, per minute, per milliliter of enzyme solution in 0.1 mol L^{-1} phosphate buffer containing $0.8 \mu\text{g L}^{-1}$ of Co(III) or Fe(III), pH 7.0, at $25 \text{ }^\circ\text{C}$. The results are shown in Tab. 3.

All enzymes were active for *n*-butanenitrile as a substrate (scaffold of aliphatic substrates **4a–d**) which revealed that all commercial NHases show catalytic activity under the reaction conditions (pH, temperature, agitation, buffer and cofactors).

Table 3. Units of enzyme activity of NHases^a from *n*-butanenitrile^b.

Entry	Nitrile hydratase	Type	U mL ^{-1c}
1	PRO-E256	Fe	881
2	PRO-E257	Co	530
3	PRO-E258	Co	554
4	PRO-E259	Co	687
5	PRO-NHASE(001)	Fe	1878
6	PRO-NHASE(002)	Co	450
7	PRO-NHASE(003)	Co	701
8	PRO-NHASE(004)	Co	1
9	PRO-NHASE(007)	Co	111
10	PRO-NHASE(008)	Co	2052
11	PRO-NHASE(009)	Fe	1338
12	PRO-NHASE(010)	Co	14
13	PRO-NHASE(011)	Co	302
14	PRO-NHASE(012)	Fe	3
15	PRO-NHASE(013)	Co	534
16	PRO-NHASE(014)	Co	1
17	PRO-NHASE(015)	Co	348
18	PRO-NHASE(016)	Co	443
19	PRO-NHASE(017)	Co	284
20	PRO-NHASE(018)	Co	>2895

^aProzomix (Prozomix, 2020); ^bgeneral conditions: *n*-butanenitrile ($14.5 \mu\text{mol}$) and $5 \mu\text{L}$ of NHase in a final volume of 1 mL with Na-phosphate buffer (0.1 mol L^{-1} , pH 7.00, containing $0.8 \mu\text{g L}^{-1}$ of Co(III) or Fe(III)) at $25 \text{ }^\circ\text{C}$, 1 min and 1000 rpm ; ^cone unit (U) was defined as the amount of the enzyme that catalyzes the conversion of $1 \mu\text{mol}$ of substrate per minute.

3.3.2 Screening of commercial NHase

All enzymatic experiments were carried out in phosphate buffered aqueous solution, using $10 \mu\text{L}$ of commercial enzyme preparation and 0.25 mmol of substrate and analyzed by GC-FID. It was observed that for *N*-derivatives of 2-oxopiperazine (substrates **4c** and **8c**) and 1-methylpiperazine (substrates **4d** and **8d**), the expected products were not formed. Moreover, the

substrate control experiment (reaction in absence of the enzyme) revealed that these substrates undergo a rapid and spontaneous decomposition by retro-Strecker reaction, leading to the formation of aldehyde and cyanide, which is an inhibitor of NHases (Yasukawa *et al.*, 2011). The results for *N*-derivatives of 2-pyrrolidinone (substrates **4a** and **8a**) and 2-piperidinone (substrates **4b** and **8b**) are shown in Tab. 4.

Table 4. Substrate conversion (**4a–b** and **8a–b**) and enantioselectivity of the commercial NHases in the hydration to **5a–b** and **9a–b**^a.

4a: R = Et, n = 1 **4b:** R = Et, n = 2
8a: R = Ph, n = 1 **8b:** R = Ph, n = 2

5a: R = Et, n = 1 **5b:** R = Et, n = 2
9a: R = Ph, n = 1 **9b:** R = Ph, n = 2

Entry	Nitrile hydratase		4a		4b		8a		8b	
	Identification	Type	Conversion ^a (%)	<i>ee</i> ^b (%)						
1	PRO-E256	Fe	n.r.	-	n.r.	-	n.r.	-	n.r.	-
2	PRO-E257	Co	1.0	n.d.	1.0	n.d.	5.2	1.0 (R)	2.2	5.2 (R)
3	PRO-E258	Co	1.2	n.d.	1.1	n.d.	10.4	2.4 (R)	5.4	7.0 (R)
4	PRO-E259	Co	4.8	17.5 (S)	1.2	n.d.	4.7	1.2 (R)	1.0	n.d.
5	PRO-NHASE(001)	Fe	n.r.	-	n.r.	-	n.r.	-	n.r.	-
6	PRO-NHASE(002)	Co	1.9	n.d.	2.4	n.d.	28.0	3.9 (R)	8.6	14.7 (R)
7	PRO-NHASE(003)	Co	1.1	n.d.	1.0	n.d.	5.2	4.3 (R)	3.0	14.5 (R)
8	PRO-NHASE(004)	Co	1.1	n.d.	1.0	n.d.	2.4	n.d.	2.3	n.d.
9	PRO-NHASE(007)	Co	n.r.	-	n.r.	-	1.4	n.d.	n.r.	-
10	PRO-NHASE(008)	Co	n.r.	-	n.r.	-	1.2	n.d.	n.r.	-
11	PRO-NHASE(009)	Fe	n.r.	-	n.r.	-	n.r.	-	n.r.	-
12	PRO-NHASE(010)	Co	32.0	1.8 (S)	n.r.	-	n.r.	-	n.r.	-
13	PRO-NHASE(011)	Co	14.2	20.6 (S)	7.1	7.9 (S)	13.5	4.9 (R)	13.4	0
14	PRO-NHASE(012)	Fe	n.r.	-	n.r.	-	n.r.	-	n.r.	-
15	PRO-NHASE(013)	Co	5.0	38.9 (S)	1.4	n.d.	3.3	2.4 (R)	4.1	n.d.
16	PRO-NHASE(014)	Co	2.4	n.d.	1.1	n.d.	14.9	8.0 (R)	18.0	3.7 (S)
17	PRO-NHASE(015)	Co	37.4	52.3 (S)	8.4	13.7 (S)	35.9	9.6 (R)	47.5	51.2 (R)
18	PRO-NHASE(016)	Co	n.r.	-	n.r.	-	3.8	n.d.	2.1	n.d.
19	PRO-NHASE(017)	Co	n.r.	-	n.r.	-	6.4	4.5 (R)	2.4	17.3 (R)
20	PRO-NHASE(018)	Co	5.6	0	2.0	n.d.	n.r.	-	1.9	n.d.

General conditions: substrate (5 μmol) and 10 μL of NHase (Prozomix, 2020) in a final volume of 1 mL with Na-phosphate buffer (0.1 mol L⁻¹, pH 7.00, containing 0.8 μg L⁻¹ of Co(III) or Fe(III)) at 25 °C, 48 h and 1000 rpm; n.r. = no reaction was observed; n.d. = not determined; ^aconversion of substrate analyzed by GC-FID; ^benantiomeric excess of product analyzed by LC-UV-CD. The *ee* and conversion are relative measurements and only chromatographic bands with a signal-to-noise ratio higher than 5:1 were considered.

The Co-type enzyme PRO-NHASE(015) showed the best performance for the conversion of all 2-pyrrolidinone and 2-piperidinone nitrile derivatives to

the corresponding amides, with highest conversion and *ee* observed for **5a**. Despite the low conversions observed, PRO-NHASE(011) and PRO-NHASE(013) accepted both aliphatic and aromatic substrates, while

PRO-NHASE(010) was selective to **4a**. On the other hand, no conversion was observed for substrates **4a**, **4b**, **8a**, and **8b**, with all four evaluated Fe-type NHases (Tab. 4, entries 1, 5, 11 and 14). These results are in accordance with the literature in which Co-type NHase has a broader substrate scope and greater activity than Fe-type NHase (Prasad and Bhalla, 2010). These differences occur because a tryptophan residue in Co-type is substituted by a tyrosine residue in Fe-type, near the active site (Kumar and Grapperhaus, 2014; Mitra and Holz, 2007). Still, Fe-type preferentially hydrate aliphatic nitriles and Co-type shows preference to aromatic nitriles (Prasad and Bhalla, 2010) and the four Fe-type used in this work indeed hydrated *n*-butanenitrile (Tab. 3).

These results from the enzymatic reactions using NHases are weak from a synthetic point of view. Although NHase is largely employed for the industrial production of acrylamide and nicotinamide (Jiao *et al.*, 2020; Wang, 2015), the application of the wild-type enzyme can be limited by its narrow substrate specificity, low enantioselectivity, unsatisfactory catalytic activity, inhibition at a high concentration of substrate and low thermostability (Bhalla *et al.*, 2018; Gong *et al.*, 2017; Prasad and Bhalla, 2010; Supreetha *et al.*, 2019; Wang, 2009). To address these issues, protein engineering is the major tool to improve nitrile hydratase features for application in organic synthesis (Wang, 2015). The biocatalytic process to produce levetiracetam **5a** is a good example. A screening was performed with approximately 30 NHases that showed low enantioselectivity and moderate conversions. The best result was obtained with the NHase from *Bradyrhizobium japonicum*, in which 20% conversion and 60% *ee* were observed. This enzyme was engineered to improve its enantioselectivity. Then, the reaction medium engineering was carried out, leading to 43% yield and 94% *ee* which was increased to > 99% *ee* upon recrystallization (Tao *et al.*, 2010).

Regarding non-engineered NHases, a recent work has studied the substrates scope of Co-type NHase from *Rhodococcus rhodochrous* ATCC BAA 870. The authors evaluated 67 substrates that differ in size from small (90 Da) to large (325 Da), in which 32 showed 50 to 100% conversion, 9 showed 16 to 50%, 5 showed 5 to 15% and 21 showed 0 to 5%. The nitrile conversion was influenced by overall size of the substrate and steric hindrance around the cyano group (Mashweu *et al.*, 2020). Other report prepared three sugar nitriles derivatives from 2-acetamido-2-deoxy- β -D-glucopyranosides and none of them was hydrated to the corresponding amide by NHase from *Rhododoccus equi* A4 (Carmona *et al.*, 2006).

Although the observed *ee* values obtained herein are still not satisfactory, all evaluated NHase showed a clear preference for (*S*) aliphatic substrates and (*R*) aromatic ones. This is a good starting point for further biocatalyst engineering (van Pelt *et al.*, 2011).

The stereoselectivity of the enzymatic conversions of compounds **4a–4b** and **8a–8b** was determined using chiral chromatography coupled with an ECD detector. The absolute configurations of the eluting enantiomers of **5b** and **9a–9b** were determined by comparing the ECD spectra obtained after trapping them in the detector with TDDFT calculations at the CAM-B3LYP/TZVP level. The calculations were carried out in order to investigate the influence of both ethyl and phenyl sidechains, as well as that of the *N*-heterocyclic substituents, on their chiroptical properties. All calculations performed for the (*S*)-configuration of **5b** and **9a–9b** resulted in a negative cotton effect at around 240 nm, which is in accordance with the literature data for levetiracetam (**5a**) (Fig. S73–S75) (Li and Si, 2011). Regarding compound **5a**, no ECD spectra were recorded, and the elution order was determined by comparing the retention times of each enantiomer with that of a commercial standard.

The PRO-NHASE(015) was selected for further investigation of medium engineering based on its best results of conversion and enantioselectivity.

3.3.3 Effect of temperature

It is well known that some NHase catalyzed reactions operate at low temperatures. The balance between reactivity and enantioselectivity for engineering the NHase from *Bradyrhizobium japonicum* conducted the final process at 4 °C, for example, in levetiracetam bioanalytical production (Tao *et al.*, 2010).

Table 5. Influence of temperature in the conversion of **4a–b** and **8a–b** into the respective amides catalyzed by PRO-NHASE(015) NHase.

Substrate	Conversion (%)	
	15 °C	25 °C
4a	5.5	37.4
4b	1.5	8.4
8a	8.0	35.9
8b	4.5	47.5

In order to explore the effect of temperature, reactions at both 15 and 25 °C were carried out in parallel and in the same experimental conditions for **4a–b** and **8a–b**. The decrease of 10 °C in the reaction temperature drastically reduced the conversion rates, as

shown in Tab. 5. Therefore, for the additional evaluated parameter, solvent effect, reactions were performed at 25 °C.

3.3.4 Effect of solvent

The control reactions experiments revealed that **4c–d** and **8c–d** undergo spontaneous decomposition by retro-Strecker reaction (section 3.3.2). As an attempt to prevent this undesired and competitive reaction, two solvent systems, which are also environmentally friendly systems, were explored—ionic liquids (IL) and polyethylene glycol (PEG).

The 1-butyl-3-methylimidazolium (BMIM) ionic liquids are the most widely used for biocatalysis and, therefore, the ILs BMIM.BF₄ (water-miscible), BMIM.PF₆ (water-immiscible) and BMIM.NTf₂ (water-immiscible) were chosen for these experiments (Cantone *et al.*, 2007). The IL system was composed of a combination of phosphate buffered solutions and increasing concentrations of the ILs BMIM.BF₄, BMIM.PF₆, and BMIM.NTf₂ in a range of 10–80% for each one. In a control experiment using substrates **4a–b** and **8a–b** and PRO-NHASE(015), no amide formation was observed and suggests that the ILs could be inhibiting the NHase activity. Interestingly, the substrates **4c–d** and **8c–d** were not decomposed in any reaction media containing ionic liquids.

The second solvent system evaluated was aqueous buffered solution with increasing concentrations of PEG₄₀₀ 10–100%. The reactions performed with substrate **4a** showed that, unlike the IL systems, the PRO-NHASE(015) was active in all proportions of PEG, even at 100%. However, the PEG significantly reduced the activity of this enzyme, with conversion decreasing from 38 to 20% in PEG₄₀₀ concentrations of 0–10%, and declining to 2% with PEG₄₀₀ concentrations higher than 50% (data not shown). In contrast to the ionic liquid system, the substrates **4c–d** and **8c–d** were decomposed in all proportions of buffer: PEG₄₀₀ and the retro-Strecker products were observed. No amide formation was detected for **4c–d** and **8c–d**.

3.4 Cholinesterases inhibition screening assays

The enzymes acetylcholinesterase (AChE) and butyrylcholinesterase (BChE) are omnipresent cholinesterases (ChE) among animals and have gained attention due to its important role in central and peripheral cholinergic neurotransmission, reducing cholinergic neuron activity, one of the event features of Alzheimer's disease (AD) (Kuca *et al.*, 2016). Epilepsy

and AD are frequently associated with neurological disorders, and both can appear simultaneously in the patient. In addition, a study reported the ameliorating of epileptic patients with nootropic effect by AChE inhibitors (Ahmad *et al.*, 2019). Similarly, brivaracetam (an analogue of levetiracetam) epilepsy drug is effective in treatment of memory impairment in AD mice (Ahmad *et al.*, 2019). Also, was demonstrated that carbamazepine, a classical antiepileptic drug, inhibited 39% AChE of brain from zebrafish (Siebel *et al.*, 2010).

The use of levetiracetam **5a** has been studied to control seizures in people with AD (Giorgi *et al.*, 2017; U.S Department of Health and Human Services, 2014). Sola *et al.* (2015) evaluated the AChE and BChE inhibitory activity of (*S*)-**5a** and it was found to be potent human acetylcholinesterase (hAChE) and human butyrylcholinesterase (hBChE) inhibitor, exhibiting IC₅₀ values of 76 and 241 nmol L⁻¹ for hAChE and hBChE, respectively, which were indirectly determined based on colorimetric assay using Ellman's reagent and thiocholine-derivatives as substrate.

In the light of this interesting dual AChE/BChE inhibitory activity, the anticholinesterase potential of the synthesized compounds **5b** and **9a–9b** were verified using the simultaneous on-flow dual parallel enzyme assay system (Seidl *et al.*, 2019). A label-free assay based on immobilized capillary enzyme reactor (ICER) allowed the direct monitoring of substrate consumption and product formation in real-time by LC-MS, employing the natural substrate of AChE, acetylcholine. Table 6 presents the inhibition percentage of all compounds tested at a concentration of 100 μmol L⁻¹, using tacrine as a positive control.

Table 6. Inhibition of eeAChE-ICER and huBChE-ICER activities by tacrine (positive control; 100 μmol L⁻¹) and *N*-heterocycles samples (100 μmol L⁻¹).

Samples	% inhibition	
	eeAChE-ICER ± SEM ^b	hBChE-ICER ± SEM ^b
Tacrine ^a	100	100
5a	10 ± 2	32 ± 2
5b	0	0
9a	5 ± 1	0
9b	10 ± 1	0

^aReference for AChE and BChE inhibition; ^bMean ± standard error of the mean (SEM, n = 2).

The racemic amides indicated low inhibitory effect when compared to tacrine, with emphasis only on **5a** that presented in increasing selectivity and potency to BChE, with 31.9% inhibition and 9.5 % for AChE.

4. Conclusions

The attempt of stereoselective synthesis of α -substituted-*N*-heterocyclic amides was demonstrated and their absolute configurations were assigned using ECD. The *N*-alkylation of 2-pyrrolidinone, 2-piperidinone, 2-oxopiperazine and 1-methylpiperazine was achieved directly from α -hydroxynitriles, which are usually either commercially available or easily prepared, thus reducing the number of synthetic steps, and minimizing the product waste. As expected, the substrate specificity varied greatly among the nitrile hydratases, highlighting the importance of the initial screening assays. The importance of amides as end products and chiral building blocks instigates the development and optimization of better biocatalysts through protein engineering to satisfactory applications in greener organic synthesis. Although the stereoselectivity was low, the products of enzymatic reactions showed a clear preference of NHases for (*S*)-aliphatic substrates and (*R*)-aromatic ones. The use of unconventional reaction media (ILs and PEG₄₀₀) that have been used successfully for many enzymes proved to be impractical for the commercial NHases used in this work. None of the racemic levetiracetam derivatives exhibit inhibitory effect on acetylcholinesterase, exemplifying the role of stereochemistry in biological activities.

Supplementary Information

Spectra (¹H NMR, ¹³C NMR, MS and IR) of all characterized compounds **2**, **3**, **4a–d**, **5a–b**, **5d**, **7**, **8a–d**, **9a–b**, and **9d**, spectra (¹H, ¹³C, ¹⁹F NMR) of the synthesized ionic liquids and the ECD figures and the lower energy conformers are available in supplementary information.

Authors' contribution

Conceptualization: Milagre, C. D. F.; Milagre, H. M. S.; Cardoso, C. L.; Batista Junior, J. M.

Data curation: Not applicable

Formal Analysis: do Amaral, B. S.; Milagre, C. D. F.; Milagre, H. M. S.; Batista Junior, J. M.; Vilela, A. F. L.; Cardoso, C. L.

Funding acquisition: Milagre, C. D. F.; Milagre, H. M. S.; Cardoso, C. L.; Batista Junior, J. M.

Investigation: do Amaral, B. S.; Vilela, A. F. L.

Methodology: Not applicable

Project administration: Milagre, C. D. F.; Milagre, H. M. S.; Cardoso, C. L.; Batista Junior, J. M.

Resources: Milagre, C. D. F.; Milagre, H. M. S.; Cardoso, C. L.; Batista Junior, J. M.

Software: Not applicable

Supervision: Milagre, C. D. F.; Milagre, H. M. S.; Cardoso, C. L.; Batista Junior, J. M.

Validation: Not applicable

Visualization: Not applicable

Writing – original draft: do Amaral, B. S.; Milagre, C. D. F.; Milagre, H. M. S.; Cardoso, C. L.; Batista Junior, J. M.

Writing – review & editing: do Amaral, B. S.; Milagre, C. D. F.; Milagre, H. M. S.

Data availability statement

All data sets were generated or analyzed in the current study.

Funding

Fundação de Amparo à Pesquisa do Estado de São Paulo (FAPESP). Grant No: 2014/50249-8; 2010/02305-5; 2013/16636-1; 2014/50926-0; 2014/25222-9; 2019/22319-5; 2019/15230-8.

Instituto Nacional de Ciência e Tecnologia INCT BioNat: Conselho Nacional de Desenvolvimento Científico e Tecnológico (CNPq). Grant No: 465637/2014-0.

Coordenação de Aperfeiçoamento de Pessoal de Nível Superior (CAPES). Finance Code 001.

Núcleo de Computação Científica (NCC/GridUNESP).

GlaxoSmithKline (GSK).

Acknowledgments

Not applicable.

References

Ahmad, G.; Rasool, N.; Rizwan, K.; Imran, I.; Zahoor, A. F.; Zubair, M.; Sadiq, A.; Rashid, U. Synthesis, *in-Vitro* Cholinesterase Inhibition, *In-Vivo* Anticonvulsant Activity And *In-Silico* Exploration of *N*-(4-methylpyridin-2-yl)thiophene-2-carboxamide analogs. *Bioorg. Chem.* **2019**, *92*, 103216. <https://doi.org/10.1016/j.bioorg.2019.103216>

Altenkämper, M.; Bechem, B.; Perruchon, J.; Heinrich, S.; Mädler, A.; Ortmann, R.; Dahse, H.-M.; Freunschdt, E.; Wang, Y.; Rath, J.; Stich, A.; Hitzler, M.; Chiba, P.; Lanzer, M.;

- Schlitzer, M. Antimalarial and antitrypanosomal activity of a series of amide and sulfonamide derivatives of a 2,5-diaminobenzophenone. *Bioorg. Med. Chem.* **2009**, *17* (22), 7690–7697. <https://doi.org/10.1016/j.bmc.2009.09.043>
- Anuradha, S.; Preeti, K. Levetiracetam with its therapeutic potentials. *Int. J. Univers. Pharm. Bio Sci.* **2013**, *2* (5), 45–58.
- Bhalla, T. C.; Kumar, V.; Kumar, V.; Thakur, N.; Savitri. Nitrile metabolizing enzymes in biocatalysis and biotransformation. *Appl. Biochem. Biotechnol.* **2018**, *185* (4), 925–946. <https://doi.org/10.1007/s12010-018-2705-7>
- Bisogno, F. R.; López-Vidal, M. G.; de Gonzalo, G. Organocatalysis and biocatalysis hand in hand: Combining catalysts in one-pot procedures. *Adv. Synth. Catal.* **2017**, *359* (12), 2026–2049. <https://doi.org/10.1002/adsc.201700158>
- Brazil. Ministério da Saúde. Portaria nº 56, de 1 de dezembro de 2017. Fica incorporado o levetiracetam para o tratamento da epilepsia, no âmbito do Sistema Único de Saúde – SUS. Brasília: Diário Oficial da União, 2017. https://bvsms.saude.gov.br/bvs/saudelegis/sctie/2017/prt0056_05_12_2017.html (accessed 2021-07-19).
- Cantone, S.; Hanefeld, U.; Basso, A. Biocatalysis in non-conventional media—ionic liquids, supercritical fluids and the gas phase. *Green Chem.* **2007**, *9* (9), 954–971. <https://doi.org/10.1039/b618893a>
- Carmona, A. T.; Fialová, P.; Křen, V.; Ettrich, R.; Martínková, L.; Moreno-Vargas, A. J.; González, C.; Robina, I. Cyanodeoxy-glycosyl derivatives as substrates for enzymatic reactions. *Eur. J. Org. Chem.* **2006**, *2006* (8), 1876–1885. <https://doi.org/10.1002/ejoc.200500755>
- Casey, M.; Leonard, J.; Lygo, B.; Procter, G. Working up the reaction. In *Advanced practical organic chemistry*; Springer, 1990; pp 141–187. <https://doi.org/10.1007/978-1-4899-6643-8>
- Chaudhry, S. A.; Jong, G.; Koren, G. The fetal safety of Levetiracetam: A systematic review. *Reprod. Toxicol.* **2014**, *46*, 40–45. <https://doi.org/10.1016/j.reprotox.2014.02.004>
- Chen, Z.; Meng, L.; Ding, Z.; Hu, J. Construction of versatile *N*-heterocycles from in situ generated 1,2-Diaza-1,3-dienes. *Curr. Org. Chem.* **2019**, *23* (2), 164–187. <https://doi.org/10.2174/1385272823666190227162840>
- Choi, I.; Chung, H.; Park, J. W.; Chung, Y. K. Active and recyclable catalytic synthesis of indoles by reductive cyclization of 2-(2-Nitroaryl)acetonitriles in the presence of Co-Rh heterobimetallic nanoparticles with atmospheric hydrogen under mild conditions. *Org. Lett.* **2016**, *18* (21), 5508–5511. <https://doi.org/10.1021/acs.orglett.6b02659>
- D’Antona, N.; Morrone, R. Biocatalysis: Green transformations of nitrile function. In *Green chemistry for environmental sustainability*; Sanjay, K., Sharma, A. M., Eds.; CRC Press - Taylor and Francis, 2010.
- Dupont, J.; Consorti, C. S.; Suarez, P. A. Z.; Souza, R. F. Preparation of 1-Butyl-3-Methyl Imidazolium-Based room temperature ionic liquids. *Org. Synth.* **2002**, *79*, 236. <https://doi.org/10.15227/orgsyn.079.0236>
- Gaussian 09*. Revision A.02; Gaussian, Inc.: Wallingford, 2016.
- Giorgi, F. S.; Guida, M.; Vergallo, A.; Bonuccelli, U.; Zaccara, G. Treatment of epilepsy in patients with Alzheimer’s disease. *Expert Rev. Neurother.* **2017**, *17* (3), 309–318. <https://doi.org/10.1080/14737175.2017.1243469>
- Gong, J.-S.; Shi, J.-S.; Lu, Z.-M.; Li, H.; Zhou, Z.-M.; Xu, Z.-H. Nitrile-converting enzymes as a tool to improve biocatalysis in organic synthesis: Recent insights and promises. *Crit. Rev. Biotechnol.* **2017**, *37* (1), 69–81. <https://doi.org/10.3109/07388551.2015.1120704>
- González-Vera, J. A.; García-López, M. T.; Herranz, R. Molecular diversity via amino acid derived α -amino nitriles: Synthesis of spirocyclic 2,6-Dioxopiperazine Derivatives. *J. Org. Chem.* **2005**, *70* (9), 3660–3666. <https://doi.org/10.1021/jo050146m>
- Hong, F.; Xia, Z.; Zhu, D.; Wu, H.; Liu, J.; Zeng, Z. *N*-terminal strategy (N1-N4) toward high performance liquid crystal materials. *Tetrahedron* **2016**, *72* (10), 1285–1292. <https://doi.org/10.1016/j.tet.2015.11.013>
- Hönig, M.; Sonderrmann, P.; Turner, N. J.; Carreira, E. M. Enantioselective chemo- and biocatalysis: Partners in retrosynthesis. *Angew. Chem. Int. Ed.* **2017**, *56* (31), 8942–8973. <https://doi.org/10.1002/anie.201612462>
- Jenner, G. Homogeneous ruthenium catalysis of *N*-alkylation of amides and lactams. *J. Mol. Catal.* **1989**, *55* (1), 241–246. [https://doi.org/10.1016/0304-5102\(89\)80257-3](https://doi.org/10.1016/0304-5102(89)80257-3)
- Jiao, S.; Li, F.; Yu, H.; Shen, Z. Advances in acrylamide bioproduction catalyzed with *Rhodococcus* cells harboring nitrile hydratase. *Appl. Microbiol. Biotechnol.* **2020**, *104*, 1001–1012. <https://doi.org/10.1007/s00253-019-10284-5>
- Kenda, B. M.; Matagne, A. C.; Talaga, P. E.; Pasau, P. M.; Differding, E.; Lallemand, B. I.; Frycia, A. M.; Moureau, F. G.; Klitgaard, H. V.; Gillard, M. R.; Fuks, B.; Michel, P. Discovery of 4-substituted pyrrolidone butanamides as new agents with significant antiepileptic activity. *J. Med. Chem.* **2004**, *47* (3), 530–549. <https://doi.org/10.1021/jm030913e>
- Krasowski, M. D.; McMillin, G. A. Advances in anti-epileptic drug testing. *Clin. Chim. Acta* **2014**, *436*, 224–236. <https://doi.org/10.1016/j.cca.2014.06.002>

- Kuca, K.; Soukup, O.; Maresova, P.; Korabecny, J.; Nepovimova, E.; Klimova, B.; Honegr, J.; Ramalho, T. C.; França, T. C. C. Current approaches against Alzheimer's disease in clinical trials. *J. Braz. Chem. Soc.* **2016**, *27* (4), 641–649. <https://doi.org/10.5935/0103-5053.20160048>
- Kumar, D.; Grapperhaus, C. A. Sulfur-oxygenation and functional models of nitrile hydratase. In *Bioinspired catalysis*; Weigand, W., Schollhammer, P., Eds.; Wiley-VCH Verlag GmbH & Co. KGaA, 2014. <https://doi.org/10.1002/9783527664160.ch12>
- Li, L.; Si, Y.-K. Study on the absolute configuration of Levetiracetam via density functional theory calculations of electronic circular dichroism and optical rotatory dispersion. *J. Pharm. Biomed. Anal.* **2011**, *56* (3), 465–470. <https://doi.org/10.1016/j.jpba.2011.07.002>
- Liu, S.; Zhao, Z.; Wang, Y. Construction of *N*-heterocycles through cyclization of tertiary amines. *Chem. Eur. J.* **2019**, *25* (10), 2423–2441 <https://doi.org/10.1002/chem.201803960>
- Lyseng-Williamson, K. A. Spotlight on Levetiracetam in epilepsy. *CNS Drugs* **2011a**, *25*, 901–905. <https://doi.org/10.2165/11208340-000000000-00000>
- Lyseng-Williamson, K. A. Levetiracetam: A review of its use in epilepsy. *Drugs* **2011b**, *71* (4), 489–514.
- Mashweu, A. R.; Chhiba-Govindjee, V. P.; Bode, M. L.; Brady, D. Substrate profiling of the cobalt nitrile hydratase from *Rhodococcus rhodochrous* ATCC BAA 870. *Molecules* **2020**, *25* (1), 238. <https://doi.org/10.3390/molecules25010238>
- Mitra, S.; Holz, R. C. Unraveling the catalytic mechanism of nitrile hydratases. *J. Biol. Chem.* **2007**, *282* (10), 7397–7404. <https://doi.org/10.1074/jbc.M604117200>
- Miyanaga, A.; Fushinobu, S.; Ito, K.; Shoun, H.; Wakagi, T. Mutational and structural analysis of cobalt-containing nitrile hydratase on substrate and metal binding. *Eur. J. Biochem.* **2004**, *271* (2), 429–438. <https://doi.org/10.1046/j.1432-1033.2003.03943.x>
- Narczyk, A.; Mrozowicz, M.; Stecko, S. Total synthesis of Levetiracetam. *Org. Biomol. Chem.* **2019**, *17* (10), 2770–2775. <https://doi.org/10.1039/C9OB00111E>
- Nelp, M. T.; Astashkin, A. V.; Brecci, L. A.; McCarty, R. M.; Bandarian, V. The alpha subunit of nitrile hydratase is sufficient for catalytic activity and post-translational modification. *Biochemistry* **2014**, *53* (24), 3990–3994. <https://doi.org/10.1021/bi500260j>
- Prasad, S.; Bhalla, T. C. Nitrile hydratases (NHases): At the interface of academia and industry. *Biotechnol. Adv.* **2010**, *28* (6), 725–741. <https://doi.org/10.1016/j.biotechadv.2010.05.020>
- Prozomix. *Enzyme Catalogue*. 2020. http://www.prozomix.com/products/listing?searchby=name&searchby_name=Nitrile+hydratase&category=21&x=53&y=3 (accessed 2020-01-27).
- Saini, M. S.; Kumar, A.; Dwivedi, J.; Singh, R. A review: Biological significances of heterocyclic compounds. *Int. J. Pharm. Sci. Res.* **2013**, *4* (3), 66–77.
- Seidl, C.; Vilela, A. F. L.; Lima, J. M.; Leme, G. M.; Cardoso, C. L. A novel on-flow mass spectrometry-based dual enzyme assay. *Anal. Chim. Acta* **2019**, *1072*, 81–86. <https://doi.org/10.1016/j.aca.2019.04.057>
- Sheldon, R. A.; Pereira, P. C. Biocatalysis engineering: The big picture. *Chem. Soc. Rev.* **2017**, *46* (10), 2678–2691. <https://doi.org/10.1039/C6CS00854B>
- Shen, Y.; Du, F.; Gao, W.; Wang, A.; Chen, C. Stereoselective nitrile hydratase. *Afr. J. Microbiol. Res.* **2012**, *6* (32), 6114–6121. <https://doi.org/10.5897/AJMR12.101>
- Siebel, A. M.; Rico, E. P.; Capiotti, K. M.; Piato, A. L.; Cusinato, C. T.; Franco, T. M. A.; Bogo, M. R.; Bonan, C. D. *In vitro* effects of antiepileptic drugs on acetylcholinesterase and ectonucleotidase activities in zebrafish (*Danio rerio*) brain. *Toxicol. Vitro* **2010**, *24* (4), 1279–1284. <https://doi.org/10.1016/j.tiv.2010.03.018>
- Sola, I.; Aso, E.; Frattini, D.; López-González, I.; Espargaró, A.; Sabaté, R.; Di Pietro, O.; Luque, F. J.; Clos, M. V.; Ferrer, I.; Muñoz-Torrero, D. Novel Levetiracetam derivatives that are effective against the alzheimer-like phenotype in mice: Synthesis, *in vitro*, *ex vivo*, and *in vivo* efficacy studies. *J. Med. Chem.* **2015**, *58* (15), 6018–6032. <https://doi.org/10.1021/acs.jmedchem.5b00624>
- Souza, R. O. M. A.; Miranda, L. S. M.; Bornscheuer, U. T. A retrosynthesis approach for biocatalysis in organic synthesis. *Chem. Eur. J.* **2017**, *23* (50), 12040–12063. <https://doi.org/10.1002/chem.201702235>
- Supreetha, K.; Rao, S. N.; Srividya, D.; Anil, H. S.; Kiran, S. Advances in cloning, structural and bioremediation aspects of nitrile hydratases. *Mol. Biol. Rep.* **2019**, *46*, 4661–4673. <https://doi.org/10.1007/s11033-019-04811-w>
- Tao, J.; Liu, J.; Chen, Z. Some recent examples in developing biocatalytic pharmaceutical processes. In *Asymmetric catalysis on industrial scale: Challenges, approaches and solutions*; Hans-Ulrich, B., Hans-Jürgen, F., Eds.; Wiley-VCH Verlag GmbH & Co. KGaA, 2010. <https://doi.org/10.1002/9783527630639.ch1>
- Tucker, J. L.; Xu, L.; Yu, W.; Scott, R. W.; Zhao, L.; Ran, N. Chemoenzymatic processes for preparation of Levetiracetam. US WO2009009117, 2009.

U.S Department of Health and Human Services, 2014. Levetiracetam for Alzheimer's disease-associated epileptiform activity. <https://www.nia.nih.gov/alzheimers/clinical-trials/levetiracetam-alzheimers-disease-associated-epileptiform-activity> (accessed 2020-04-29).

UCB. 2018 Full Year Results. UCB https://www.ucb.com/_up/ucb_com_ir/documents/2018_FY_results_presentation_-_final.pdf (accessed 2020-01-17).

Uges, J. W. F.; Vecht, C, J. Levetiracetam. In *Atlas of Epilepsies*; Panayiotopoulos, C. P., Ed.; Springer London, 2010. https://doi.org/10.1007/978-1-84882-128-6_271

van Pelt, S.; Zhang, M.; Otten, L. G.; Holt, J.; Sorokin, D. Y.; van Rantwijk, F.; Black, G. W.; Perry, J. J.; Sheldon, R. A. Probing the enantioselectivity of a diverse group of purified cobalt-centred nitrile hydratases. *Org. Biomol. Chem.* **2011**, *9* (8), 3011–3019. <https://doi.org/10.1039/c0ob01067g>

Vilela, A. F. L.; Seidl, C.; Lima, J. M.; Cardoso, C. L. An improved immobilized enzyme reactor-mass spectrometry-based label free assay for butyrylcholinesterase ligand screening. *Anal. Biochem.* **2018**, *549*, 53–57. <https://doi.org/10.1016/j.ab.2018.03.012>

Wang, M.-X. Progress of enantioselective nitrile biotransformations in organic synthesis. *CHIMIA International Journal for Chemistry* **2009**, *63* (6), 331–333. <https://doi.org/10.2533/chimia.2009.331>

Wang, M.-X. Enantioselective biotransformations of nitriles in organic synthesis. *Acc. Chem. Res.* **2015**, *48* (3), 602–611. <https://doi.org/10.1021/ar500406s>

Wen, Y.; Liang, M.; Wang, Y.; Ren, W.; Lü, X. Perfectly green organocatalysis: Quaternary ammonium base triggered cyanosilylation of aldehydes. *Chinese J. Chem.* **2012**, *30* (9), 2109–2114. <https://doi.org/10.1002/cjoc.201200598>

Yasukawa, K.; Hasemi, R.; Asano, Y. Dynamic kinetic resolution of α -aminonitriles to form chiral α -amino acids. *Adv. Synth. Catal.* **2011**, *353* (13), 2328–2332. <https://doi.org/10.1002/adsc.201100360>.

Young, S. D.; Buse, C. T.; Heathcock, C. H. 2-Methyl-2-(Trimethylsiloxy)Pentan-3-one. In *Organic Syntheses*; John Wiley & Sons, 2003. <https://doi.org/10.1002/0471264180.os063.09>

Zhang, J.; Wang, H.; Ma, Y.; Wang, Y.; Zhou, Z.; Tang, C. CaF₂ Catalyzed S_N2 type chlorodehydroxylation of chiral secondary alcohols with thionyl chloride: A practical and convenient approach for the preparation of optically active chloroalkanes. *Tetrahedron Lett.* **2013**, *54* (18), 2261–2263. <https://doi.org/10.1016/j.tetlet.2013.02.079>